**RESEARCH ARTICLE**

# Performance Analysis of Skin Contact Wearable Textile Antenna in Human Sweat Environment

**D. RAM SANDEEP**[1], **B. T. P. MADHAV**[2], **SUDIPTA DAS**[3],
**NIAMAT HUSSAIN**[4], **(Member, IEEE), TANVIR ISLAM**[5], **AND MOATH ALATHBAH**[6]

[1]Department of Electronics and Communication Engineering, Raghu Engineering College, Visakhapatnam, Andhra Pradesh 531162, India
[2]Department of Electronics and Communication Engineering, ALRC-R&D, Koneru Lakshmaiah Education Foundation (KLEF), Guntur, Andhra Pradesh 522302, India
[3]Department of Electronics and Communication Engineering, IMPS College of Engineering and Technology, Malda, West Bengal 732103, India
[4]Department of Intelligent Mechatronics Engineering, Sejong University, Seoul 05006, South Korea
[5]Department of Electrical and Computer Engineering, University of Houston, Houston, TX 77204, USA
[6]Department of Electrical Engineering, College of Engineering, King Saud University, Riyadh 11421, Saudi Arabia

Corresponding authors: Niamat Hussain (niamathussain@sejong.ac.kr) and Moath Alathbah (malathbah@ksu.edu.sa)

**ABSTRACT** This work evaluates the performance of a triple-frequency operating circularly polarized wearable jute textile antenna in a human body sweat environment. The propounded antenna is designed to operate on the human body. So, contact with human skin allows the antenna to absorb the eccrine gland-rich mineral secretion (sweat) in regular use. The absorbed fluid alters the fabric substrate's dielectric properties, ultimately leading to changes in the antenna performance. For that purpose, the antenna's jute fabric is examined in a scanning electron microscope (SEM) and optical electron microscope to observe its water absorption characteristics in the wet state. An artificial sweat solution that closely mimics natural human sweat was taken in all the experimental conditions (The Pickering Laboratories'-Artificial Eccrine Perspiration). The present work addresses the antenna's performance regarding operating frequencies, axial ratios, efficiency, and gains in three different sweat absorbency environments, i.e., exposure to light spray, partial exposure, and complete absorbency conditions. The antenna's lifetime in the sweat environment was also inspected in an electrochemical workstation. The antenna's conformal analysis shows that it retains its optimal performance both in normal and bending conditions. The results from all these analyses confirm the robust functionality of the textile antenna in human sweat conditions.

**INDEX TERMS** Jute antenna, dielectric property, scanning electron microscope, optical-electronic microscope, artificial sweat solution, wearable antenna.

## I. INTRODUCTION

Wearable technologies are the most important ones that can significantly change our lives. They have been widely used in diverse fields, including entertainment, sports, military, education, and healthcare. At an instant, in the healthcare sector, wearable devices are used to monitor human physiologies like step count, temperature, calories burned, blood pressure, glucose levels, and heart rate [1]. Among such devices, textile patch antennas have a unique role; textile antennas (textenna) are exclusive antennas, fundamentally made up of fabric materials [2]. In comparison, the conventional ones are made up of rigid materials. Textile antennas can be easily attached to the user's garments; they are lightweight, compact, outwardly unnoticeable, and flexible. Textile antennas are fabricated using various methods, such as screen printing [3], inkjet printing [4], and stitching or embroidery [5]. The circular polarization (CP) characteristics in textile antennas make communication far more effective. Since the CP antennas don't need any particular orientation between the receiving and transmitting antennas, they also have resistance to signal degradation because of adverse

The associate editor coordinating the review of this manuscript and approving it for publication was Tutku Karacolak.

weather conditions [6]. Abundant literature has been available on the recently developed textile antennas on various textile substrates such as denim textile [7], polyester fabric [8], and other fabrics [9], [10], [11], [12].

As a piece of the user's clothing, these antennas are frequently exposed to human sweat, potentially altering the antenna's resonating performance. There is some literature on the textile antenna's performance in tap water and other humid environments [13], [14], [15], [16], [17], [18], [19], where most of the textile antenna's performance is considerably varied. However, minimal research has been reported investigating human sweat's effects on antenna performance, such as operating frequencies, axial ratios, and gain. Keeping in view of diverse real-time applications in the field of medicine and defense, the need for evolving a robust natural fibre-based circularly polarized antenna design is found essential. It's found that minimal research has been done in the field of designing a natural fibre-based textile antenna that allows on-body communication with circular polarization characteristics even under complete sweat absorbency circumstances. Moreover, the antenna's lifetime is also examined in a human sweat environment using an electrochemical workstation for the first time in this work.

This article is structured as follows; section II briefly describes the antenna design, materials, and fabrication methodology. Section III evaluates the textenna performance in different human sweat environments. Section IV presents a discussion on bending analysis. Section V analyses electrochemical behavior. Section VI of the article demonstrates performance comparison and finally, the conclusion is summarized in section VII.

## II. WEARABLE JUTE ANTENNA DESIGN

The antenna derived its basic design from a sickle shape and is fed with a microstrip feed line. The ground plane also includes a similar sickle-shaped structure that was introduced to facilitate the necessary 90 degrees phase shift for CP at the operating frequencies and is placed opposite to an elliptical form [20].

As illustrated in Fig. 1(a), the sickle-shaped structures in the patch and ground are derived gradually from a 7 mm radius (R1) circular structure that initially functions at 4.9 GHz frequency. In the next step, as illustrated in Fig. 1(b), the whole circular forms in the patch and ground plane are transformed into half-circular forms with a semi-elliptical base that enables this structure to function at 3.1, 4.9, and 6.6 GHz frequencies.

Further, as shown in Fig. 1(c), another curvature with half of the radius of $R_1$ is taken, and affix thus formed semi-curvatures inversely opposite to the prime curvature. At the same time, a rectangular stub was placed on the semi-elliptical base, which ultimately facilitates function at 3.5, 4.9 and 5.8 GHz frequencies, respectively.

The ground and patch element's conductivity are materialized using industrial-grade copper paint (Caswell- copper conductive paint, the surface resistivity of <1 Ohm/sq at 1 mil
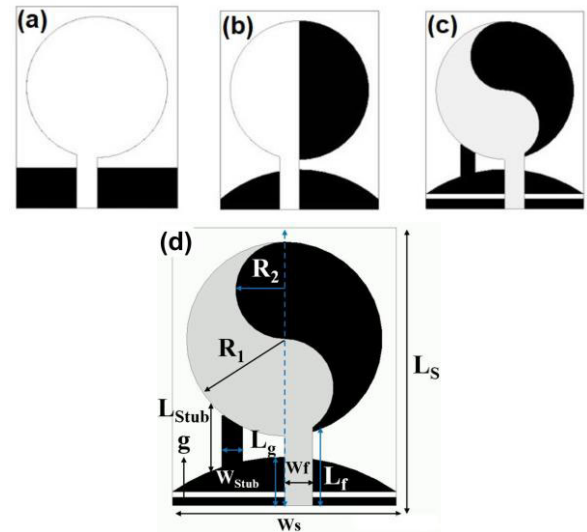


**FIGURE 1.** The schematics of the wearable jute antenna: (a) design step-1, (b) design step-2, (c) design step-3 and (d) complete geometric view.

thickness). The antennas model, along with the geometry, is shown in Fig. 1(d). The complete dimensions of the proposed textenna in mm are as: Ls = 20, Ws = 16, $L_{stub}$ = 2.5, $W_{stub}$ = 1.5, g = 0.5, $R_1$ = 7, $L_f$ = 5, $W_f$ = 2, $R_2$ = 3.5, $L_g$ = 2.5, (all units in mm).

### A. EFFECTS OF THE STUB ON CIRCULAR POLARIZATION

The key parameter which is crucial to achieving CP in the resonating frequencies is the stub and its length ($L_{stub}$). Fig. 2a depicts the impact of the stub on circular polarization. As seen in iteration-2 (Fig. 2a), the axial ratio values are not less than 3dB without the stub. However, when the stub was introduced, the axial ratio values at the operating frequencies fell under 3 dB. An axial ratio value of less than 3 dB indicates that the ratio of the major and minor axis of the polarization ellipse is almost circular. Hence the stub plays a significant role in determining the desired characteristics and ensuring proper circular polarization at operating frequencies.

It is a well-known fact that the sharp points obviously attract the charges towards them and accumulate in huge concentrations. This same phenomenon works on the sharp points of the sickle-shaped radiating and ground elements that have the tendency to attract charges towards them from the broader areas. So, this attraction of charges makes them move through the sickle-shaped radiating and ground elements in a circular motion, leading to CP at 3.5, 4.9, and 5.8 GHz successively.

As illustrated in Fig. 2(b), the proposed model resonates (|S11| < −10 dB) in triple frequencies of 3.5, 4.9, and 5.8 GHz. The axial ratio curves indicate that the suggested antenna offers circular polarization over all the operating bands. The prototype is fabricated on jute material and is also illustrated in Fig. 2(c). A decent match has been noted
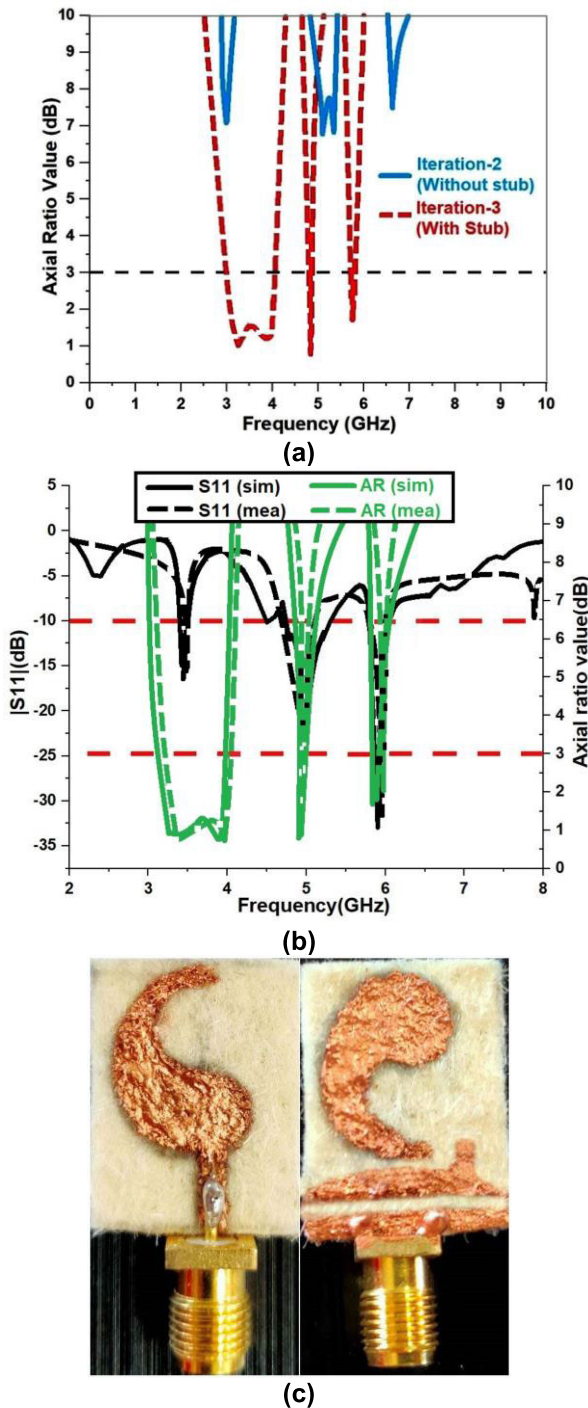
**FIGURE 2.** The proposed antennas (a) axial ratio for various design steps, (b) |$S_{11}$| and axial ratio plot and (c) prototype.

between the simulations and measurements of the resonating frequencies and axial ratios.

## B. RADIATION PATTERNS (CO AND CROSS POLARIZATION)

In circularly polarized antennas, the radiation pattern consists of two orthogonal polarizations: right-hand circular polar-
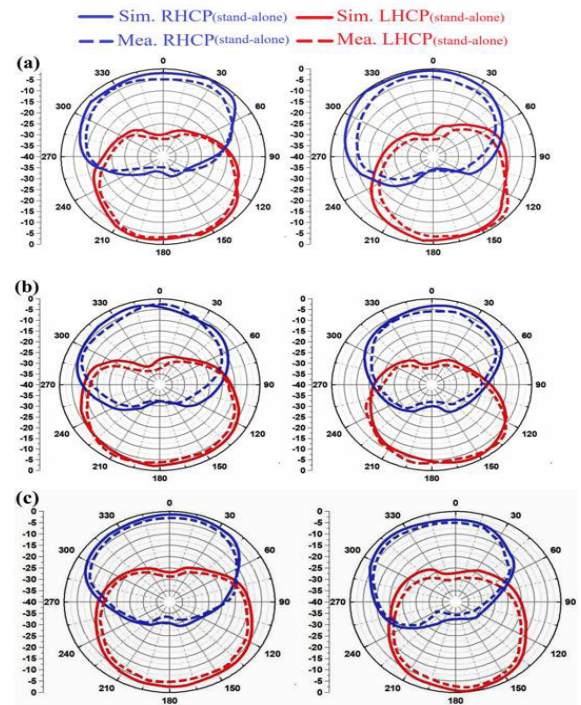


**FIGURE 3.** Simulated and measured radiation patterns in stand-alone conditions at (a) 3.5, (b) 4.9, and (c) 5.8 GHz.

ization (RHCP) and left-hand circular polarization (LHCP). When a circularly polarized antenna is transmitting or receiving RHCP signals, the RHCP component represents co-polarization, while the LHCP component represents cross-polarization. Similarly, when dealing with LHCP signals, the LHCP component represents co-polarization, and the RHCP component represents cross-polarization.

The proposed textenna's radiation characteristics were validated in an anechoic chamber in free space conditions. Fig. 3 shows the LHCP and RHCP patterns at the three operating frequencies in the two principal planes ($\varphi = 0$ degrees, $\varphi = 90$ degrees).

## III. SWEAT CONDITIONS

Sweating is a thermoregulatory mechanism that cools down the body temperature if it's getting too hot. It happens by evaporative cooling of the eccrine glands' water-rich secretion. An adult's maximum sweating rate ranges between 10–14 liters per day or 2–4 liters per hour. Hot weather, physical exercise, emotional stress, and sometimes fever associated with illness stimulates sweating. The propounded textenna is so developed to function in proximity with human skin, so it must work in different on-body circumstances. When the textenna gets in contact with human sweat, its performance is altered due to the conductive nature of human sweat.

The proposed antenna is built on the Jute material, which falls under the lignocellulosic fiber, wherein the lignin component of these fibers is highly hydrophobic. So, unlike other natural cellulosic fibers such as cotton, jute doesn't absorb
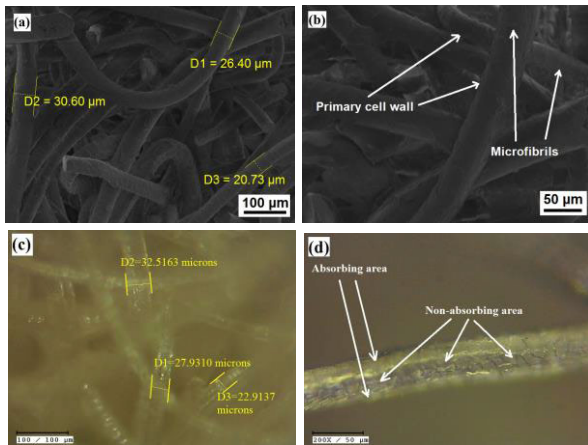
**FIGURE 4.** The jute material SEM analysis in the typical dry state at (a) 100$\mu$m, (b) 50$\mu$m, and optical microscope analysis in wet state at (c) 100$\mu$m, and (d) 50$\mu$m.

uniformly around its fiber structure. Fig. 4(a-b) shows the scanning electron microscope (VEGA3; TESCAN) images of the jute fibers at 100 and 50 micrometer depth. As in Fig. 4(a), a precise and proper intervention of fibers is seen in a resolution of 100 micrometers, where fibers' diameters are also shown. In a resolution of 50 micrometers in Fig. 4(b), the jute fibers microfibrils and the primary cell wall are evident. The microfibrils are made up of cellulose, a key polymeric structural component that provides strength and structural stability to the fibers and is responsible for the jute fibers' robust nature.

To examine the absorbency characteristics, the jute material is placed in the artificial eccrine perspiration for 24 hours and analyzed in an optical microscope. As shown in Fig. 4(c), the diameter of the fibers is also not varying much due to the absorption. The analyses shown in Fig. 4(d) conclude that the absorbency is not uniform across the fibers. This is a good advantage because the absorbance is low when compared to other cellulosic fibers like cotton. Fig. 5(a) shows the scanning electron microscope images of the cotton fibers at 100 micrometers depth. Where the diameters of the cotton fibers vary from 10–55 micrometers. The cotton textile is placed in the sweat solution for 24 hours and analyzed in an optical microscope to examine the absorbency characteristics. As shown in Fig. 5(b), the diameters of the cotton fibers are varied largely. As a cellulosic fiber, uniform absorbency characteristics can also be seen in Fig. 5(c). The proposed textena's performance is experimentally tested in different sweat conditions, by a light spray, a partial exposure and a complete absorbency condition in artificial eccrine perspiration. In all these cases, anechoic chamber measurements are taken for the validation of the designed antenna.

## A. ARTIFICIAL ECCRINE PERSPIRATION
An artificial sweat solution (The Pickering Laboratories'- Artificial Eccrine Perspiration) was used in all the experimentation conditions. It's an artificial solution [21] that

closely resembles human eccrine sweat, and its chemical composition is in no way different from the actual human sweat. It contains four most abundant metabolites (Ammonia, Lactic acid, Urea, Uric acid), seven most abundant minerals (Chloride, Magnesium, Iron, Zinc, Sodium, Nitrate, Potassium, Calcium, and Copper sulfate), nineteen amino acids (Taurine, L-Threonine, L-Valine, L-Serine (Largest Amount), L-Tyrosine, L-Leucine, L-Phenylalanine, L-Methionine, L-Histidine, L-Lysine, L-Isoleucine, L-Ornithine, L-Glutamic Acid, L-Alanine, L-Asparagine, L-Citrulline, L-Aspartic Acid, L-Arginine, Glycine), and a pH of 4.5. Typically, sweat is a transparent biofluid with low tonicity and a slightly acidic pH. The artificial sweat solution contains the four most abundant metabolites and nineteen amino acids, which work together to maintain an identical pH value to real human sweat.

## B. A LIGHT SPRAY OF SWEAT SOLUTION
The fabricated prototype weighed in different sweat exposure conditions is shown in Fig. 6. The antenna's initial weight in normal dry conditions is 0.3558 grams. It was measured using a high-precision weighing machine (Make; Ohaus). The texteena was exposed to a light spray (aerosol) of artificial sweat. The solution was sprayed 15 times; then, it was kept rested for a few minutes to allow the antenna for full absorbency. The textena's weight increased to 0.3783 grams. The percentage increase in its weight is 6.32 %, which is a minimal absorbency case.

### 1) RESONATING FREQUENCIES
As demonstrated in Fig. 7(a), there were no major deviations in the operating frequencies. The antenna is functioning normally in all three operating frequencies, as in the complete dry state, but a slight change in the lower operating frequencies' bandwidth is observed. Initially, it was 3.4–3.5 GHz; now, it is operating from 3.3–3.6 GHz. The return loss value at 4.9 GHz frequency is also increased to −26 dB from −24dB. Excluding these, there were no variations reported in the 5.8 GHz frequency. The measurement setup is shown in Fig. 8(a).

### 2) AXIAL RATIOS, GAIN, AND EFFICIENCY
The circular polarization characteristic is also verified, as shown in Fig. 7(a). The axial ratios in the operating bands are under the 3 dB line ranging from 3.2–3.7, 4.7–4.98, and 5.7–6.1. So, all these bands are operating with the CP radiation. The gain value in the operating bands is 5, 8.9, and 9.1 dBi. The efficiency in the above frequencies ranges from 81–90%, as shown in Fig. 7(d).

## C. A LIGHT DIP IN SWEAT SOLUTION
For more time, if the proposed textena was kept in contact with the human body, it absorbed more sweat due to adsorption. The jute material is a densely felted fabric, so it initially adsorbs the liquids rather than absorption. This case is ideally equal to partial absorption on its surface. The material antenna is partially contacted by the artificial sweat solution
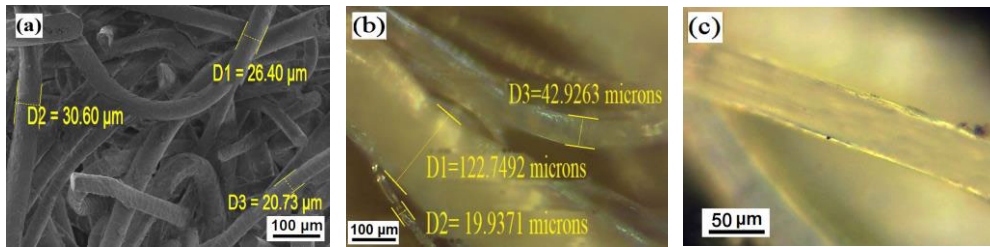
**FIGURE 5.** The cotton material SEM analysis in the typical dry state at (a)100$\mu$m, and optical microscope analysis in wet state at (b) 100$\mu$m, and (c) 50$\mu$m.
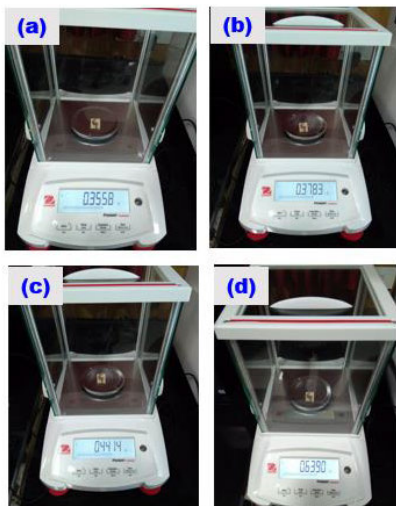


**FIGURE 6.** Photographs of the antenna while weighted in different sweat exposure conditions: (a) normal dry state, (b) light spray exposure, (c) partial exposure, and (d) full absorbency case.

for a few minutes and weighed in the weighing machine. As illustrated in Fig. 6 (c), the antenna weight after partial exposure is 0.4414 grams and gained 0.0856 grams. The percentage increase in the weight was 24.05 %, and then it was tested in an anechoic chamber.

### 1) RESONATING FREQUENCIES
The results from Fig. 7(b) show some minor variation in the resonating frequencies. Though the antenna is in contact with the artificial sweat solution, it didn't absorb the solution completely. In this condition, the antenna showed good resistance to the above moisture condition. The return loss of the lower operating frequency, 3.5 GHz, was reduced to −14 dB, and its bandwidth was also reduced to normal dry conditions. A slight enhancement in the 4.9 GHz frequencies bandwidth is reported. Excluding that, there were no significant variations observed in the other operating frequency of 5.8 GHz, as illustrated in Fig. 8(b).

### 2) AXIAL RATIOS, GAIN, AND EFFICIENCY
As shown in Fig. 7(b), slight variations in the axial ratio bandwidth are reported in the lower band (3.23–3.65). The

other two bands are generally working as in a normal dry state. The gain values at the operating bands are 4.1, 8.1, 8.8 dBi, and the efficiency in the above frequencies ranges from 80-88 %, as illustrated in Fig. 7 (d).

### D. COMPLETE ABSORBENCY IN THE SWEAT SOLUTION
The textenna is dipped in the sweat solution for 24 hours. The complete immersion facilitates the fibers to absorb the sweat fluid completely. The prototype antenna was again weighted as seen in Fig. 6d, and its value is 0.6390 grams; the percentage increase in its weight is 79.58 %.

### 1) RESONATING FREQUENCIES
When tested in the anechoic chamber, a lower operating band rejection was reported at 3.5 GHz in the complete absorbency condition. Though the antenna completely absorbs the sweat fluid, the other two frequencies still work relatively well with minor variations in their bandwidth (4.6-5.5 and 5.5-6.3 GHz), as seen in Fig. 7c. The measurement setup is shown in Fig. 8c.

### 2) AXIAL RATIOS, GAIN, AND EFFICIENCY
The circular polarization is also verified; with the changes in resonating frequencies, the axial ratios follow the same shift with a band rejection at a 3.5 GHz frequency, as shown in Fig. 7c. The gain and efficiency curves are shown in Fig. 7d. The measured gain value in the operating bands are 8.4 and 8.6 dBi, and the efficiency in the above frequencies are 79–87 %.

### E. COTTON TEXTILE ANTENNA PERFORMANCE
The absorption characteristic of the fiber plays a crucial role in deciding the antenna performance in wet conditions. For instance, if the same design is developed on a cellulosic fiber material (cotton), its resonating characteristics are drastically varied even if it got exposed to a partial or complete sweat environment. The cotton antenna resonates at 4.6 GHz frequency in normal dry conditions. However, when exposed to a moderate sweat environment, it's completely rejecting the operating band, as seen in Fig. 9 (a–b). Compared with other natural materials like cotton, jute fiber exhibits good robustness against moisture even in complete absorbency conditions.
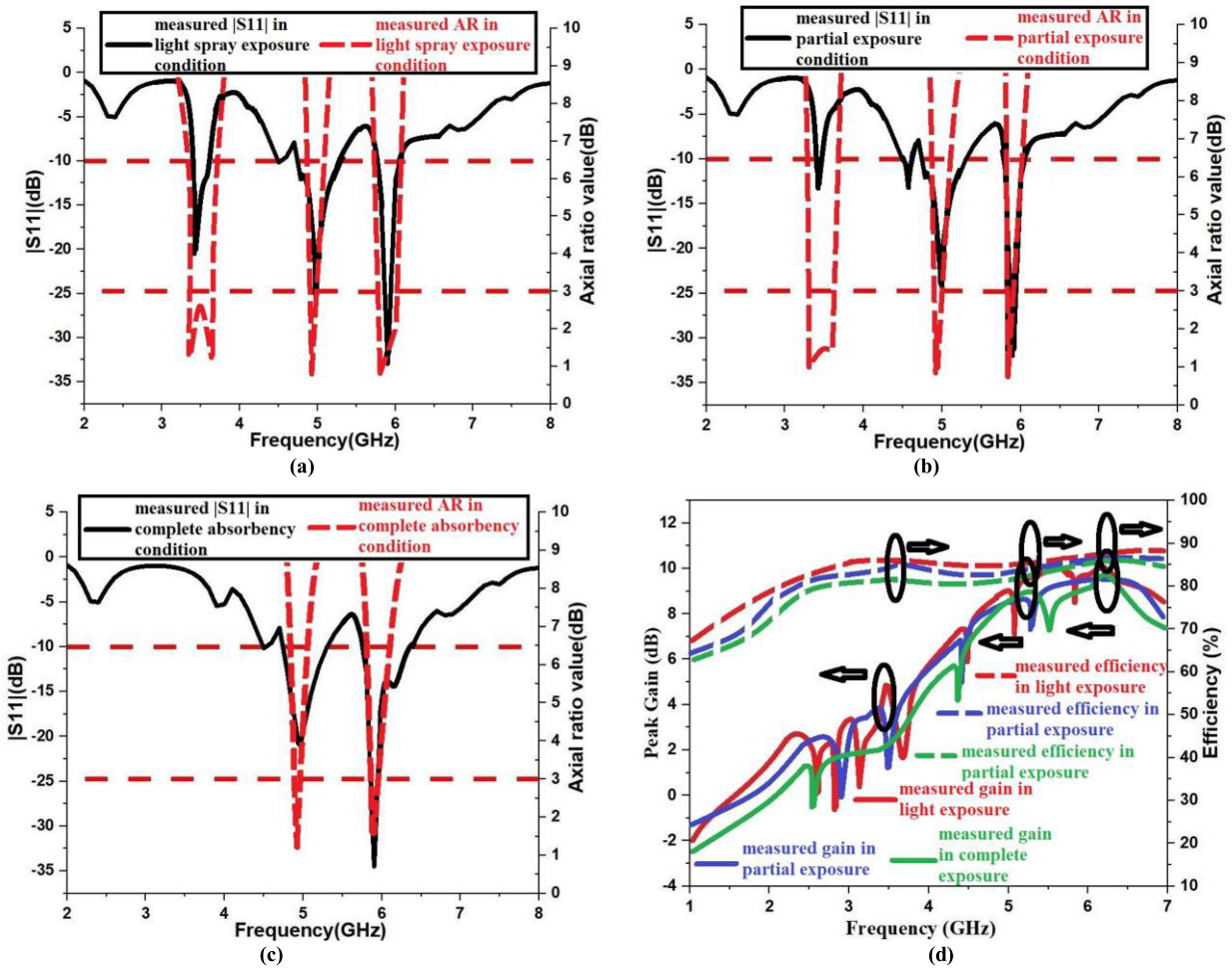
**FIGURE 7.** Measured |S$_{11}$| and axial ratios in different conditions (a) light spray exposure, (b) partial exposure, (c) complete absorbency, and (d) measured gain and efficiency in all three cases.
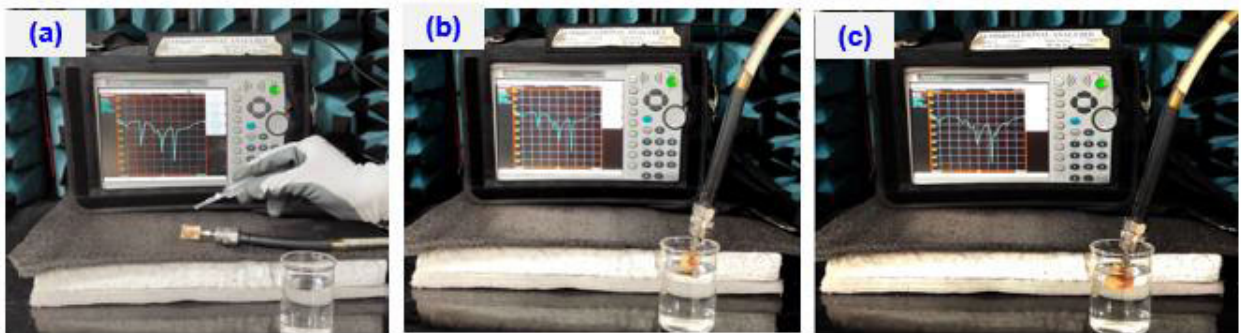


**FIGURE 8.** Measurement setup of the jute antenna in different environments (a) light spray exposure, (b) partial exposure, (c) complete absorbency.

### F. REAL TIME MEASUREMENTS

The practical experiment was conducted in low, moderate, and hyper levels of real exasperating conditions. The developed jute antenna is placed on the subject's clothing to enable the absorption of human sweat. The three exposure conditions, such as little spray, moderate exposure and complete

absorbency conditions, are practically achieved by increasing the exposure time of the antenna in actual sweat conditions. The antenna weights in all three real-time sweat absorbency conditions are carefully matched with those obtained in artificial sweat absorbency conditions. Then the antenna is tested in an anechoic chamber, as illustrated in Fig. 10(a–c).
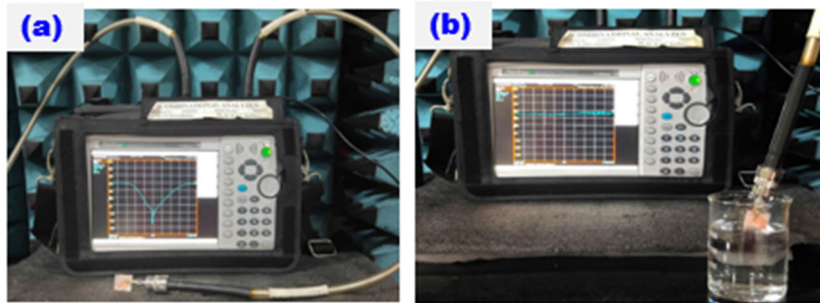
**FIGURE 9.** Measurement setup of the cotton antenna in (a) dry condition and (b) partial exposure to sweat solution.



**FIGURE 10.** Measurement setup of the jute textenna in different on body human sweat environments (a) little exposure, (b) partial exposure, (c) complete absorbency.

The obtained results are in good agreement with the results obtained from the artificial eccrine perspiration solution. To investigate the effect of multiple sweat exposures on antenna performance. It was duly administered at all levels of exposure for 50 repetitions/cycles. The results thus securely concluded that there aren't considerable variations in resonating characteristics observed while performing the same experiment multiple times.

## IV. BENDING ANALYSIS
Bending analysis is performed in wearable antennas to understand and evaluate the performance and reliability of the antenna when subjected to bending or flexing due to the movements and deformations of the human body. Wearable antennas are designed to be integrated into clothing or worn on the body, and they need to withstand the mechanical stresses and strains associated with body movements. To examine the effect of bending radii on the |S11| was examined by bending the antenna in both x- and y-direction. The antenna's curvature while bending is entirely guided by the bending angle. It can be explained as the curvature angle devised by molding the textenna's substrate over a cylindrical form of radius Rc. Equation. 1 is used to calculate the cylindrical form bending radius through the bending angle. For a texteena with unique proportions, every bending angle $\theta$ produces an individual bending radius.

$$Rc = \frac{(L_s \times 360°)}{(\theta \times 2\pi)} \quad (1)$$

where $L_s$ indicates the length of the substrate.

In this study, two kinds of bending aspects are examined. They are defined as (1) vertical dimension bending (bending in terms of length, i.e., x-direction) and (2) horizontal dimension bending (bending in terms of width, i.e., y-direction bending). The bending angle differed from 0 to 45 degrees in both cases. A maximum bending angle of 45 degrees is considered because for an antenna with a dimension of $20 \times 16$ mm$^2$, a 45-degree bend is quite enough to adapt to any human body surface. The 45-degree bending test reflects the range of bending that textile antennas may experience during severe usage. When integrated into clothing, antennas can be subjected to various bending angles due to body movements or interactions with the environment. Hence testing antennas at 45 degrees provides a reasonable approximation of these real-world scenarios.

### A. VERTICAL BENDING ANALYSIS
If the antenna is bent in its length dimension, then it's classified as vertical bending or x-direction bending. The below section evaluates the proposed textenna's vertical flexible behavior through bending in the x-direction at different bending angles with a step size of 15 degrees. The bending analysis are shown with 15 degrees, 30 degrees and 45 degrees bending angles as shown in Fig. 11 (a–c).

The textenna was bent at 15 degrees along the length dimension, the operating frequencies moved towards the upper-frequency ranges and resonated at 3.55, 5.0, and 5.9 GHz, as shown in Fig. 11(d).

The textenna has undergone 30-degree vertical bending, the resonating frequencies shift more on the way to the upper
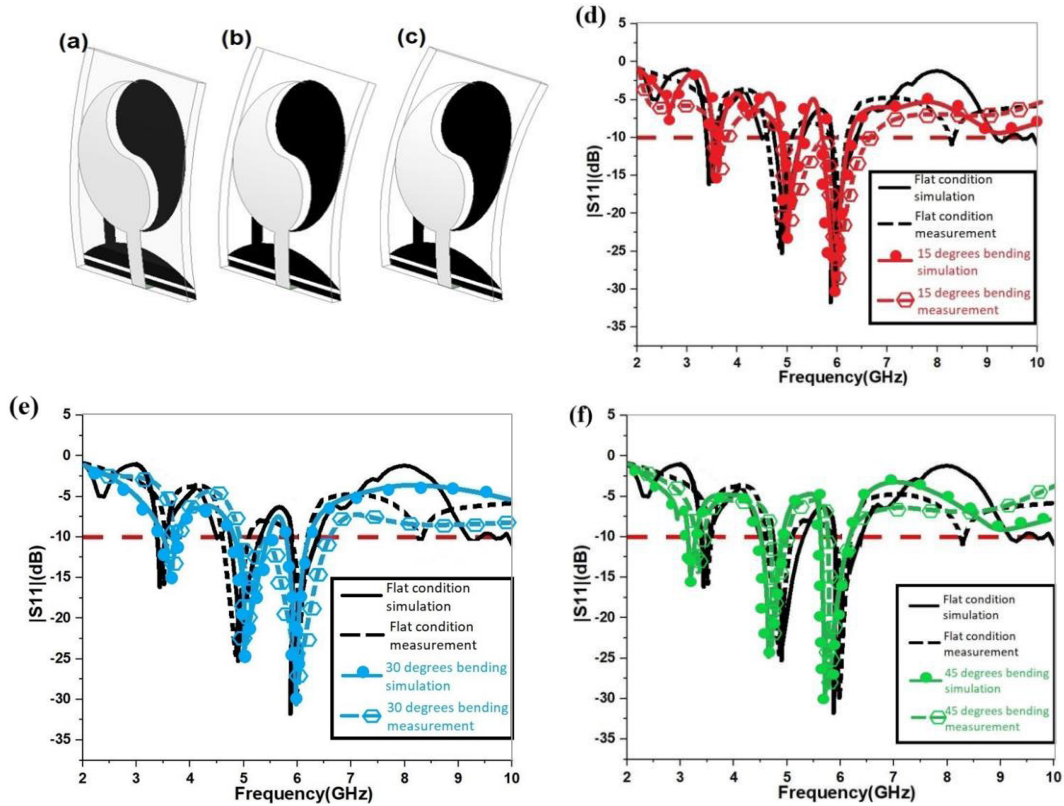
**FIGURE 11.** The proposed antennas' x-axis bending at (a) 15 °, (b) 30 °, (c) 45 ° and its |S11| at various bending angles at (d) 15 °, (e) 30 °, (f) 45 °.

frequencies. They resonated at 3.60, 5.10, and 6.05 GHz, as illustrated in Fig. 11(e). Similarly, when the textenna was bent vertically at 45 degrees, the resonating frequencies shifted to lower frequencies and resonated at 3.4, 4.6, and 5.6 GHz, as shown in Fig. 11(f). Up to a 30-degree vertical bending state, they shifted to upper bands; beyond that, they moved on the way to lower bands. The textenna showed insignificant resonance changes when contrasted to the flat state. The above bending conditions observe an utmost +/− 0.30 GHz frequency shift to higher and lower frequencies. However, they fall under the ranges of WLAN, WIMAX, and ISM band.

### B. HORIZONTAL BENDING ANALYSIS

If the antenna is bent in its width dimension, then it's classified as horizontal bending or y-direction bending. The section below evaluates the proposed textenna's horizontal flexible behavior through bending horizontally at different (15, 30, and 45 degrees) angles as shown in Fig. 12 (a–c).

When the textenna was bent horizontally 15 degrees, the operating bands experienced a slight shift towards lower frequencies, resonating at 3.38, 4.74, and 5.74 GHz, respectively, as shown in Fig. 12(d). While for bending angle of 30 degrees, the resonating frequencies underwent further downward, operating at 3.3, 4.7, and 5.7 GHz, respectively., as depicted in Fig. 12(e). When the antenna was further bent

at 45 degrees horizontally, as opposed to 15 and 30-degree horizontal bending angles, the resonating bands are moved prone to higher frequencies and resonated at 3.7, 5.1, and 6.0 GHz, respectively (Fig. 12(f)).

The bending analysis shows that vertical bending generates up to +/− 0.3 GHz of normalized frequency shift, and the horizontal bending effects are less than +/− 0.2 GHz. This is because x-directional bending particularly impacts the resonance path more than y-directional bending, especially for the fundamental resonance mode.

## V. ELECTROCHEMICAL BEHAVIOR ANALYSIS

The conductive layers of the proposed antenna are realized by brush paintable copper paint. Thus, formed conductive layers, when gets in contact with human sweat, react with these rich mineral and amino acid fluids, leading to the decay of the copper. This natural process that happens over time is called corrosion. "It is an electrochemical or chemical reaction between a material (metal) and its environment that results in a deterioration of the material and its properties (American Society for Testing and Materials (ASTM) G-15)" [22]. Traditionally corrosion is measured by placing the test specimen in the open atmosphere or respective media. This traditional procedure takes many months to find the corrosion rate, so many electrochemical techniques are proposed to measure the corrosion rate instantly. They are executed very fast and
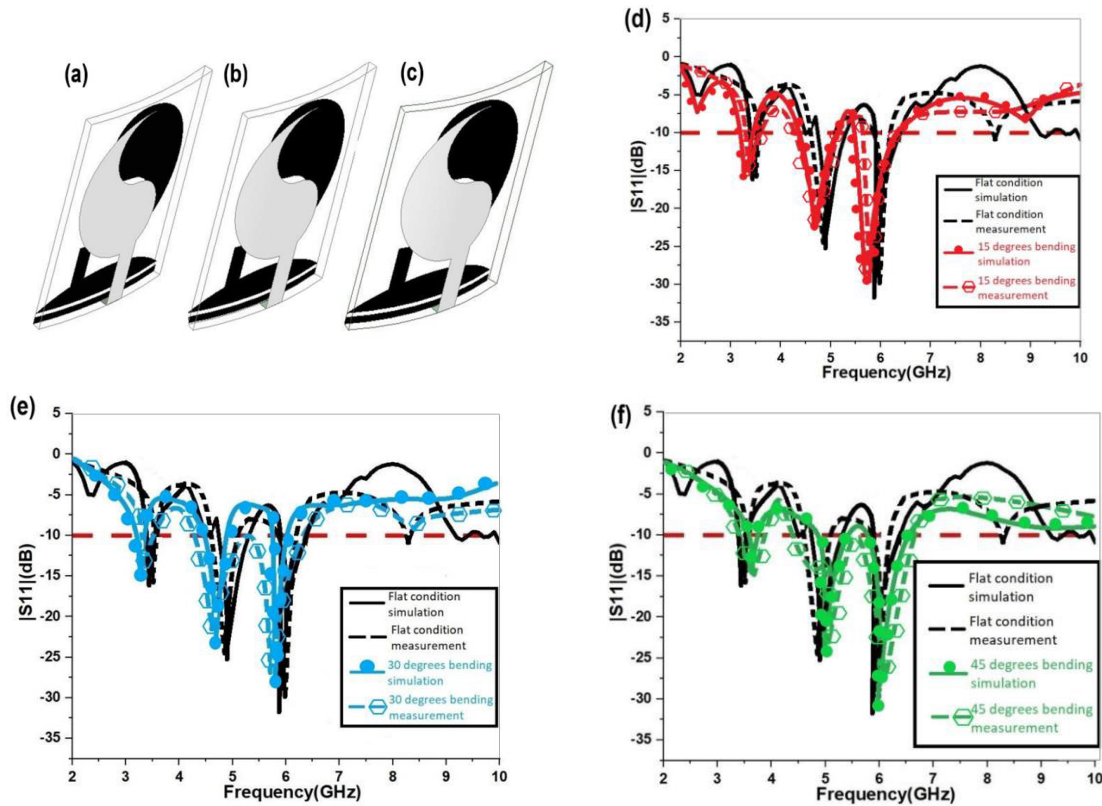
**FIGURE 12.** The proposed antennas' y-axis bending at (a) 15 °, (b) 30 °, (c) 45 ° and its |S11| at various bending angles at (d) 15 °, (e) 30 °, (f) 45 °.

**TABLE 1.** Performance comparison of the proposed wearable jute antenna with related state-of-the-art works.

| Reference antennas | Antenna Dimensions (mm$^2$) and substrate material | Functioning frequencies in the dry state (GHz) | Functioning frequencies in a complete wet state (GHz) | CP and antenna lifetime calculation in wet conditions |
|---|---|---|---|---|
| [14] | Ballistic textile | 1.6 | 0.9 | (Yes/No) |
| [15] | 70×85 (felt) | 2.4 | Complete band rejection | No |
| [17] | 125×65 (fleece) | 2.25–2.75 | Complete band rejection | No |
| [18] | 60×45 (fleece) | 2.45 | 1.4 | No |
| [19] | 63×60 (cotton) | 3.1–10.6 | Reduction in bandwidth for partial exposure | No |
| **This work** | **20×16 (treated jute fabric)** | **3.5, 4.9, 5.8** | **4.9, 5.8** | **Yes** |

are sensitive. Corrosion is caused by a redox reaction, such as in equation (2). So, the use of electrochemical methods is obvious because corrosion is an electrochemical process.

$$Fe \rightarrow Fe^{2+} + 2e^- \tag{2}$$

Fundamentally, corrosion is a prolonged process, so the typical rate is indicated by milli inches per year (mpy) or millimeters per year (mmpy). The flat corrosion cell of the electrochemical apparatus polarizes the test specimens to stimulate the corrosion process and make measurements in a

few minutes. Thus, the electrochemical instruments instantly measure the corrosion rate even at a very low corrosion value. As illustrated in Fig. 13(a), France made SP-(Biologic SAS) electrochemical workstation is employed to obtain the antenna's corrosion rate. The textenna was placed in the flat corrosion cell of the electrochemical workstation. The artificial eccrine perspiration solution is taken as the electrolyte inside the corrosion cell. Fig. 13(b) shows the Tafels plot curve obtained in the experimentation, used to find the specimen's Tafels slopes and corrosion rate. It was drawn

(a)
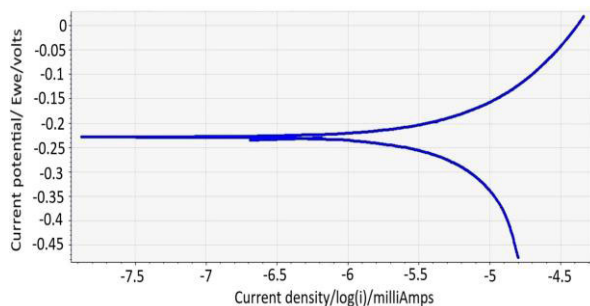


(b)

**FIGURE 13.** Measurement setup (a) the electrochemical workstation with flat corrosion cell, and (b) Tafel plot curve in artificial sweat conditions.

between the corrosion current potential (Ecorr) and current density (Icorr).

The corrosion occurs distinctively at a rate regulated by an equilibrium between opposing electrochemical reactions. These opposing reactions can be seen in Tafel's plot. The curve represents, towards the bottom is a cathodic reaction (reduction reaction) wherein the electrolyte detaches the electrons from the metal surface. Here, in this reaction, the flow of electrons is always from the metal surface to the electrolyte. The other curve represents, towards the top is an anodic reaction, wherein the metal is oxidized by the gaining of electrons from the electrolyte. The sum of cathodic and anodic currents gives rise to the total current, which is measured by sweeping the potential of the metal with the electrochemical workstation. The keen point in the tafels plot is the point where the polarity of the current reverses as the reaction changes from cathodic to anodic or anodic to cathodic. Plotting this point on the vertical scale gives the Ecorr value of the test specimen. Icorr is obtained by extrapolating the extended linear portions of cathodic and anodic curves back to their converging point. From thus derived values, the potentiostat of the electrochemical workstation renders the corrosion rate in mmpy. In normal conditions, the antenna's measured corrosion rate is 0.00001142 mmpy, and similarly, in sweat conditions, the rate is 0.008195 mmpy. On comparing these corrosion values, it is concluded that there is a minimal variation found in the corrosion rate under sweat conditions. So, the antenna can withstand a harsh body sweat environment.

## VI. PERFORMANCE COMPARISON

Although there is not much research reported on the performance evaluation of textile antennas in sweat conditions, a comparative analysis has been made on the available work of textile antennas in complete wet conditions, as given in Table 1. Thanks to the treated jute fabric, the proposed wearable antenna has a stable function in a wet state, with the advantage of compact size and a greater number of operating bands. To the best of the author's knowledge, this is the only study where the CP performance and lifetime calculation of any antenna in wet conditions has been performed.

## VII. CONCLUSION

An In-Vitro examination for performance analysis of a circularly polarized jute textenna in human body sweat conditions is done in this study. The jute material absorption characteristics were analyzed with a scanning electron microscope and an optical electron microscope. In a typical dry state, the developed antenna resonated at triple frequencies of 3.5, 4.9, and 5.8 GHz in WLAN, Wi-Max, and ISM band applications. For evaluating its performance in the on-body sweat conditions, an artificial sweat solution was used. The antenna was thoroughly investigated in the anechoic chamber in different sweat environments, such as exposure to (i) a light spray of sweat solution, (ii) a partial dip in the sweat solution, and (iii) a complete absorbency condition where the proposed antenna is wholly dipped in the artificial sweat solution. The antenna's resonating frequencies, gain, axial ratios, and efficiency were measured in all the above cases. The antenna usually functioned with slight variations in the resonating frequencies and axial ratios in the first two conditions. However, a band rejection was observed when completely exposed to the sweat solution for 24 hours. A similar kind of action has also been observed in the axial ratios of the proposed antenna. The above analysis concludes that the 4.9 and 5.8 GHz frequencies work uninterrupted in all sweat absorbency conditions. The antenna's lifetime was also evaluated in an electrochemical workstation, which shows its least degrading nature in a sweat environment. These real-time measurements from the anechoic chamber and electrochemical workstation validate the antenna's applicability for on-body communication at Wi-Max and ISM band applications.

## REFERENCES

[1] J. J. Rutherford, "Wearable technology," *IEEE Eng. Med. Biol. Mag.*, vol. 29, no. 3, pp. 19–24, May 2010.

[2] K. N. Paracha, S. K. Abdul Rahim, P. J. Soh, and M. Khalily, "Wearable antennas: A review of materials, structures, and innovative features for autonomous communication and sensing," *IEEE Access*, vol. 7, pp. 56694–56712, 2019.

[3] I. Martinez, C. Mao, D. Vital, H. Shahariar, D. H. Werner, J. S. Jur, and S. Bhardwaj, "Compact, low-profile and robust textile antennas with improved bandwidth for easy garment integration," *IEEE Access*, vol. 8, pp. 77490–77500, 2020.

[4] M. Akbari, M. W. A. Khan, M. Hasani, T. Björninen, L. Sydänheimo, and L. Ukkonen, "Fabrication and characterization of graphene antenna for low-cost and environmentally friendly RFID tags," *IEEE Antennas Wireless Propag. Lett.*, vol. 15, pp. 1569–1572, 2016.

[5] A. Tsolis, W. Whittow, A. Alexandridis, and J. Vardaxoglou, "Embroidery and related manufacturing techniques for wearable antennas: Challenges and opportunities," *Electronics*, vol. 3, no. 2, pp. 314–338, May 2014.

[6] S. Sarkar and B. Gupta, "A dual-band circularly polarized antenna with a dual-band AMC reflector for RFID readers," *IEEE Antennas Wireless Propag. Lett.*, vol. 19, no. 5, pp. 796–800, May 2020.

[7] D. Ferreira, P. Pires, R. Rodrigues, and R. F. S. Caldeirinha, "Wearable textile antennas: Examining the effect of bending on their performance," *IEEE Antennas Propag. Mag.*, vol. 59, no. 3, pp. 54–59, Jun. 2017.

[8] Roshni, S. Babu, M. P. Jayakrishnan, P. Mohanan, and K. P. Surendran, "Design and fabrication of an E-shaped wearable textile antenna on PVB-coated hydrophobic polyester fabric," *Smart Mater. Struct.*, vol. 26, no. 10, Oct. 2017, Art. no. 105011.

[9] K. Masrakin, H. A. Rahim, P. J. Soh, M. Abdulmalek, I. Adam, M. N. B. M. Warip, Q. H. Abbasi, and X. Yang, "Assessment of Worn textile antennas' exposure on the physiological parameters and well-being of adults," *IEEE Access*, vol. 7, pp. 98946–98958, 2019.

[10] K. Zhang, P. J. Soh, and S. Yan, "Design of a compact dual-band textile antenna based on metasurface," *IEEE Trans. Biomed. Circuits Syst.*, vol. 16, no. 2, pp. 211–221, Apr. 2022.

[11] J. Zhong, A. Kiourti, T. Sebastian, Y. Bayram, and J. L. Volakis, "Conformal load-bearing spiral antenna on conductive textile threads," *IEEE Antennas Wireless Propag. Lett.*, vol. 16, pp. 230–233, 2017.

[12] D. R. Sandeep, N. Prabakaran, B. T. P. Madhav, K. L. Narayana, and Y. P. Reddy, "Semicircular shape hybrid reconfigurable antenna on jute textile for ISM, Wi-Fi, Wi-MAX, and W-LAN applications," *Int. J. RF Microw. Comput.-Aided Eng.*, vol. 30, no. 11, Nov. 2020, Art. no. e22401.

[13] H. Shahariar, H. Soewardiman, C. A. Muchler, J. J. Adams, and J. S. Jur, "Porous textile antenna designs for improved wearability," *Smart Mater. Struct.*, vol. 27, no. 4, Apr. 2018, Art. no. 045008.

[14] T. Kaija, J. Lilja, and P. Salonen, "Exposing textile antennas for harsh environment," in *Proc. MILCOM Mil. Commun. Conf.*, Oct. 2010, pp. 737–742.

[15] R. Sanchez-Montero, P.-L. Lopez-Espi, C. Alen-Cordero, and J.-A. Martinez-Rojas, "Bend and moisture effects on the performance of a U-shaped slotted wearable antenna for off-body communications in an industrial scientific medical (ISM) 2.4 GHz band," *Sensors*, vol. 19, no. 8, p. 1804, Apr. 2019.

[16] P. M. Potey and K. R. Tuckley, "Variation in properties of wearable textile antennas due to sweat in erratic climatic conditions," in *Proc. Loughborough Antennas Propag. Conf. (LAPC)*, Nov. 2018, pp. 1–6.

[17] H.-S. Zhang, S.-L. Chai, K. Xiao, and L. F. Ye, "Numerical and experimental analysis of wideband E-shape patch textile antenna," *Prog. Electromagn. Res. C*, vol. 45, pp. 163–178, 2013.

[18] K. Kamardin, M. K. A. Rahim, P. S. Hall, N. A. Samsuri, T. A. Latef, and M. H. Ullah, "Planar textile antennas with artificial magnetic conductor for body-centric communications," *Appl. Phys. A, Solids Surf.*, vol. 122, no. 4, pp. 1–9, Mar. 2016.

[19] M. S. Shakhirul, M. Jusoh, A. Sahadah, C. M. Nor, and H. A. Rahim, "Embroidered wearable textile antenna on bending and wet performances for UWB reception," *Microw. Opt. Technol. Lett.*, vol. 56, no. 9, pp. 2158–2163, Sep. 2014.

[20] D. Ram Sandeep, N. Prabakaran, B. T. P. Madhav, K. L. Narayana, and P. Rakesh Kumar, "Systematic investigation from material characterization to modeling of jute-substrate-based conformal circularly polarized wearable antenna," *J. Electron. Mater.*, vol. 49, no. 12, pp. 7292–7307, Oct. 2020.

[21] C. J. Harvey, R. F. LeBouf, and A. B. Stefaniak, "Formulation and stability of a novel artificial human sweat under conditions of storage and use," *Toxicology Vitro*, vol. 24, no. 6, pp. 1790–1796, Sep. 2010.

[22] R. W. Revi and H. H. Uhlig, *Corrosion and Corrosion Control: An Introduction to Corrosion Science and Engineering*. Hoboken, NJ, USA: Wiley, 2008.

**D. RAM SANDEEP** received the Ph.D. degree in wearable antennas from KLEF, in 2022. Currently, he is an Associate Professor with the Department of Electronics and Communication Engineering, Raghu Engineering College, Andhra Pradesh, India. He has contributed over 30 research articles in peer-reviewed journals and international conferences. His research interests include implantable and medical antennas, remote healthcare technologies, body-centric wireless sensors, flexible textile antennas, multi-band reconfigurable textennas, MIMO antennas, optimization of microwave circuits, device modeling, the IoT, wireless communications, biomedical engineering, and allied fields. He is also associated with different international journals as an editorial board member.

**B. T. P. MADHAV** is a Professor and the Director of research and development with KLEF. He has published over 527 articles in international and national journals and conferences. Scopus and SCI publications of 379 with an H-index of 33 and total citations of more than 3980. He has authored 20 books and published 12 patents. His research interests include antennas, liquid crystal applications, and wireless communications. He received several awards, such as the World Record for the Highest Number of Publications under Age 40 years, the Indian Book of Records, the Asian Book of Records, the Outstanding Reviewer from Elsevier, the Best Researcher and a Distinguished Researcher from KLEF. He also received the Best Teacher Award from KLEF, in 2011, 2012, 2013, 2014, 2015, 2016, 2017, 2018, and 2019. His name was included in Top 2% scientists of the world, published by Stanford University in collaboration with Elsevier. He has guided seven Ph.D. scholars for award; and three Ph.D. scholars submitted thesis and six scholars pursuing Ph.D. degree under his guidance. He is a reviewer of several international journals, including IEEE, Elsevier, Springer, Wiley, and Taylor and Francis; and several international conferences.

**SUDIPTA DAS** received the Ph.D. degree from the University of Kalyani, India, in 2017. He is currently an Associate Professor with the Department of Electronics and Communication Engineering, IMPS College of Engineering and Technology, West Bengal, India. He has 13 years of teaching and ten years of research experience. He has contributed more than 150 research articles in various peer-reviewed international journals and conferences of repute. He has authored one book on microstrip filter design, and edited four books on THz technology and also contributed several book chapters. His research interests include design and development of microstrip antennas for microwave, mm-wave and THz communication systems, flexible antenna design, implantable antenna, filter design, meta-material, FSS, RFID, microwave components, and THz systems. He received the Outstanding Teacher in Electronics and Communication Engineering Award by the Global Outreach Research and Education Summit Awards, in 2019. He is an active reviewer of several international journals of IEEE, Elsevier, Springer, Wiley, Taylor and Francis, MDPI, and IOP Science. His name was listed in Marquis Who's who in the World in 2016. He is associated with different international journals as an editorial board member.

**NIAMAT HUSSAIN** (Member, IEEE) received the B.S. degree in electronics engineering from the Dawood University of Engineering and Technology, in 2014, the M.S. degree in electrical and computer engineering from Ajou University, Suwon, South Korea, and the Ph.D. degree in information and communication engineering from Chungbuk National University, Cheongju, South Korea, in 2021. Currently, he is an Assistant Professor of intelligent mechatronics engineering with Sejong University, Seoul, South Korea. He has authored/coauthored more than 70 international journal articles. His research is mainly focused on meta-material antennas, the IoT antennas, mm-wave antennas, wireless power transfer, and bioelectromagnetics. He received the Best Paper Award for his paper presented at the Korea Winter Conference (KIEES), in 2017. He was a recipient of the Outstanding Graduate Researcher Award. In 2021 and 2022, he was featured as the World's Top 2% Scientists, ranked by Stanford University in collaboration with Elsevier.

**MOATH ALATHBAH** received the B.Sc. degree from Liverpool University, U.K., the M.Sc. degree from Glasgow University, U.K., and the Ph.D. degree from Cardiff University, U.K. He is currently an Assistant Professor with King Saud University, Saudi Arabia, and a Transitional Postdoctoral Researcher with Cardiff University. His research interests include the development of photoelectronic, integrated electronic active and passive discrete devices, the design, fabrication, and characterization of RF and THz components, and MMIC design employing nitride-based III–V semiconductors by means of micro and nano technology.

● ● ●

**TANVIR ISLAM** is a Research Assistant with the Department of Electrical and Computer Engineering, University of Houston, Houston, TX, USA. His current research interests include printed antennas, biomedical implantable antennas, radars, microwave passive components, electromagnetics, and bio-electromagnetics in the field of MRI safety, especially the RF-induced heating for various medical applications. He is actively engaged with various professional societies as a member. He is an active reviewer of different international journals.